Flowslide Triggering in Volcanic Soils: Role of Stratigraphy and Bedrock Exfiltration

José J. Lizárraga, Ph.D.;[1] Xiang Li;[2] and Giuseppe Buscarnera, Ph.D., M.ASCE[3]

[1]Department of Civil and Environmental Engineering, Northwestern University, 2145 Sheridan Road, Evanston, IL 60208-3109; e-mail: jjlizarraga@u,northwestern.edu
[2]Department of Civil and Environmental Engineering, Northwestern University, 2145 Sheridan Road, Evanston, IL 60208-3109; e-mail: xiangli2.2015@u.northwestern.edu
[3]Associate Professor, Department of Civil and Environmental Engineering, Northwestern University, 2145 Sheridan Road, Evanston, IL 60208-3109 (corresponding author); e-mail: g-buscarnera@northwestern.edu

ABSTRACT

Rainfall-induced landslides pose significant risks to urban communities and infrastructure. The combination of transient rainfall, unsaturated soil properties, and spatially varying topography makes them difficult to forecast over large areas. This contribution describes a computational framework to evaluate landslide susceptibility over regional landscapes. To this aim, a description of a case study is presented, in which more than forty shallow flowslides were triggered after 48-hr of continuous precipitation over a region of 9 km^2. Several hypotheses have been proposed to explain the widespread distribution of slope instabilities, such as soil liquefaction, pore pressure pulses due to layering, bedrock exfiltration, and antecedent hydrologic conditions, among others. Here, by using available field and laboratory data to constrain the input parameters, different model scenarios are tested to back-analyze the spatial and temporal occurrence of the events, namely, i) slope failure caused by infiltration in homogenous deposits, ii) failures mediated by permeability contrasts in heterogeneous slopes, and iii) slope instabilities caused by bedrock springs within homogeneous soil profiles. Each scenario is evaluated by comparing the computed susceptibility maps and the temporal evolution of unstable areas against the landslide inventory. It is shown that stratigraphy effects can capture successfully the observed distribution of landslide source areas. Lastly, the advantages and limitations of each scenario are discussed, and recommendations for future analyses are proposed.

INTRODUCTION

Rainfall-induced landslides are a major hazard in tropical and mountainous areas due to their high spatial and temporal frequencies (Petley, 2012). In this context, landslide susceptibility zonation becomes an important tool for risk management, especially for densely populated urban settings affected by such phenomena.

During the last decades, significant advances have been made in the development of spatially-distributed models for landslide susceptibility (Godt et al., 2008; Montgomery and Dietrich, 1994). These models map across a regional landscape the areas that can become unstable under the effect of heavy rainfalls. Due to the large spatial extension of these problems, the simulation of the infiltration process often relies on the assumption of homogeneous soil profiles to compute the evolution of pore pressures, which are then coupled with suction-dependent soil strength criteria

to define slope stability thresholds. Thus, a missing element in most of such modelling frameworks is the presence of layered profiles, which can alter the timing and location of landslide triggering. This contribution describes the application of a spatially-distributed model to evaluate landslide susceptibility over landscapes characterized by layered slopes. To this aim, a brief description of a case study is first presented. By using available field and laboratory data to constrain the input parameters, three model scenarios are tested to back-analyze the spatial and temporal occurrence of the events. Each scenario is evaluated by comparing computed susceptibility maps and temporal evolution of unstable area against documented data. Lastly, advantages and limitations of each scenario are discussed.

CASE STUDY

The study area covers a region of 9 km^2 within the Pizzo d'Alvano massif (Campania, southern Italy) (Figure 1). Detailed analyses of the meteorological characteristics of the event, geological and geotechnical properties of the deposits and groundwater regime have been documented elsewhere (Cascini et al., 2011; Crosta and Dal Negro, 2003; Guadagno et al., 2005). Here only a brief description of the site-specific input datasets used for the simulations is presented.
Due to the proximity to the Somma-Vesuvius volcanic system, the geologic setting is characterized by unsaturated pyroclastic sediments loosely-deposited over a fractured carbonate bedrock (Cascini et al., 2008). As a result of previous volcanic eruptions, alternations of ashes (with thickness between 40 to 60 cm) and pumices (10 to 30 cm) are often found, resulting in stratified profiles across the landscape (Crosta and Dal Negro, 2003). The thickness of the deposits varies according to elevation, particularly, the depth to bedrock increases from the crest (about 0.5–2m) to the toe of the massif (several meters) (De Vita et al., 2006).

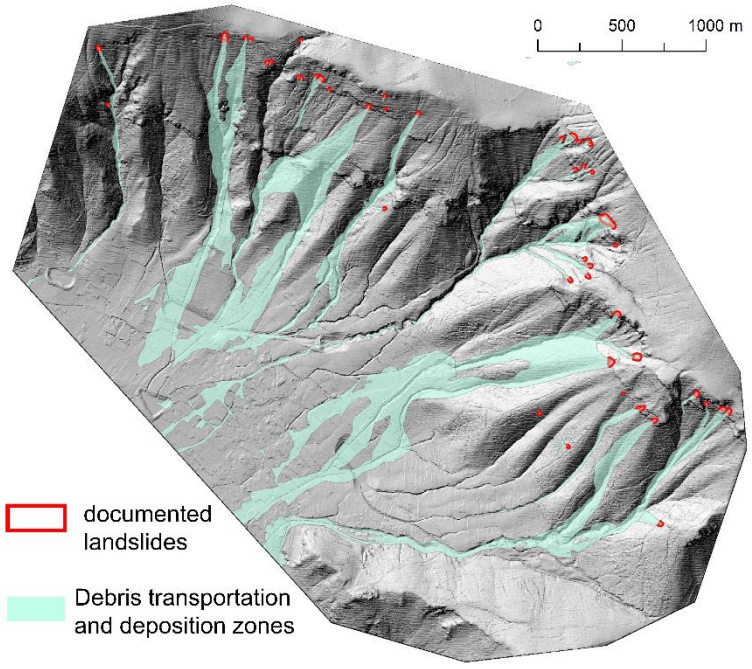

Figure 1. Study area and spatial distribution of documented landslides

On May 4-5 of 1998, after 48 hr of continuous precipitation, more than a hundred shallow landslides occurred over an area of 60 km^2, with 47 of them located in the study area (Figure 1, red contours). Most slope instabilities originated at inclinations between 33° and 50°, with failure depths between 0.5 and 2.0 m. Cumulated rainfall of 180 mm was reported at the closest meteorological station (located 4.5 km from the study site) by the end of the storm. Landslide triggering started in the late afternoon of May 5th, during the last 12 hours of the event.

Several hypotheses have been proposed to explain the widespread distribution of shallow slope failures. For instance, Cascini et al., (2003), identified the location of ephemeral bedrock springs and measured the flow rate after major rainfall events. Figure 2 shows their results for three distinct locations, five months (starting in October 1998) after the occurrence of the May 4-5 landslides. Such considerations were used to suggest that bedrock exfiltration played an important role on the observed distribution of landslide triggering. Alternatively, Mancarella et al. (2012), based on results of column infiltration tests in layered profiles, showed that sharp decreases in matric suction could develop as a result of high contrasts on values of hydraulic conductivity *K*. Such results along with the widespread presence of layered deposits were used to suggest that stratigraphy alone was mostly responsible for the development of shallow failures. In the following, after a brief description of the model formulation, these scenarios (i.e., triggering controlled by layering or bedrock exfiltration, respectively) will be used to back-analyze the available evidence.

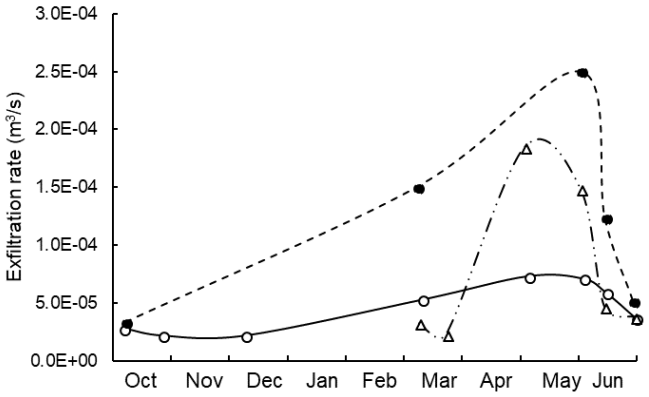

Figure 2. Measured exfiltration rate at three locations following the May 4-5 events in 1998.

MODEL DESCRIPTION AND INPUT DATA

The spatially-distributed model relies on a vectorized Finite Element (FE) algorithm that solves simultaneously the governing equations for unsaturated flow at multiple slope units sharing the same discretization parameters (i.e., mesh size and time steps). Hereafter only a brief description of the implementation procedures is presented, while more details of the formulation can be found in Lizárraga and Buscarnera (2018).

The model is implemented in three stages: *pre-processing, computation*, and *postprocessing* (Figure 3). The *input* stage requires the discretization of the zone of study into slope units. For the present case, a Digital Elevation Model (DEM) with a resolution of 2x2m is used. Spatially-distributed input datasets are treated as georeferenced grids and are superposed on the background

DEM using a Geographical Information System (GIS). Spatially varying initial/boundary conditions and discretization parameters are also required.
During the *computation* stage, the calculated pore pressures are used to update the FS (Factor of Safety, derived based on infinite slope assumption) at each cell throughout the landscape. If at any time step, a value of FS<1 is detected, then the corresponding time and depth of failure for that cell are stored, otherwise, a non-data index is assigned. The *output* stage consists on the generation of landslide susceptibility maps at selected times and their visualization in a GIS platform.

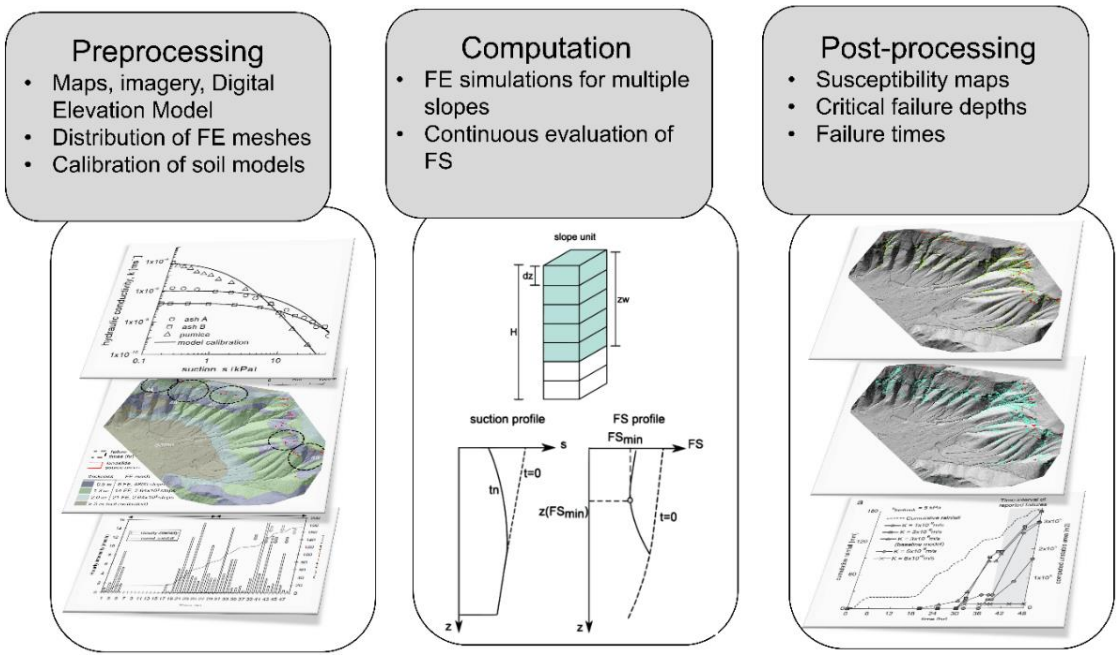

Figure 3. Schematic representation of model workflow

For the present case study, hydrological and soil strength data were available for each of the layers (Bilotta et al., 2005). Due to the widespread prevalence of shallow failures, the assumption of infinite slope is used. The spatial distribution of soil thickness was based on Cascini et al., (2011). Initial suction conditions were derived from field monitoring data for an instrumented hillslope (Pirone et al., 2015), which suggested linear suction (s) profiles with values of s = 20 kPa at the soil-bedrock interface (Cascini and Sorbino, 2003). Rainfall data measured at the closest station is used (Frattini et al., 2004). Further details can be found in Lizárraga et al. (2017).
To illustrate the hydrologic response of a typical unsaturated layered slope, a numerical simulation of transient infiltration in layered and homogeneous columns are presented. Figure 4 shows a schematic representation of the model discretization, initial and boundary conditions. The simplified profile is based on average values of layer thickness reported by Crosta and Dal Negro (2003). Water Retention Curves (WRC) and Hydraulic Conductivity Functions (HCF) for each layer based on the Van Genuchten model were calibrated using laboratory data (Bilotta et al., 2005). It should be noted that the pumice layers (poorly-graded, gravel-sand mixtures) are much more permeable than the ashes (silty sands), with values of K up to three orders of magnitude higher than ash B (Crosta and Dal Negro, 2003).

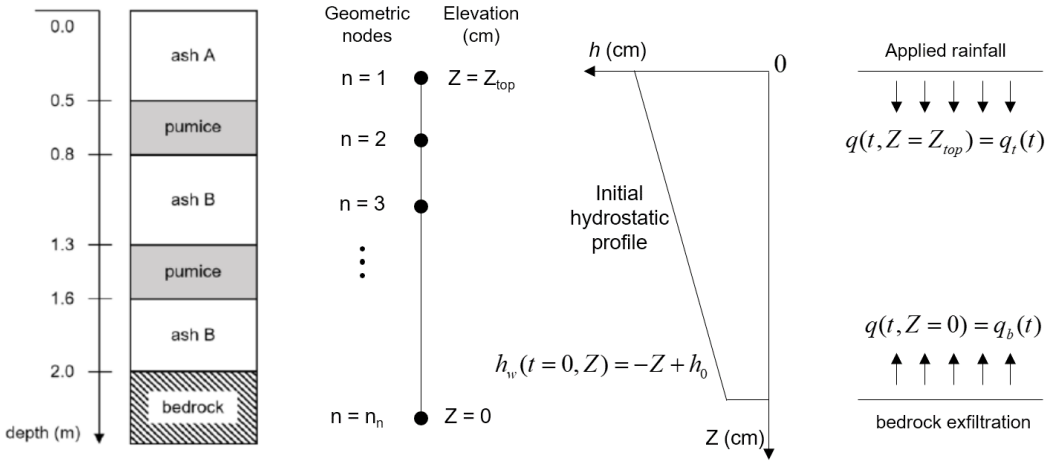

Figure 4. Numerical model for transient infiltration in a layered soil profile.

Three simulations are performed, all subjected to the same measured rainfall history and initial conditions. Model **H1** consists of a homogeneous profile (with parameters corresponding to those of ash B due to its larger thickness). Model **L** is based on the layered system shown in Figure 4, while model **H2** is similar to scenario **H1** but with a bedrock exfiltration rate equal to $q_b = 2 \times 10^{-4}$ $m^3 s^{-1}$ (i.e., the highest value reported in Figure 2) applied at the base during the last 10 hours of the storm (Cascini et al., 2003).

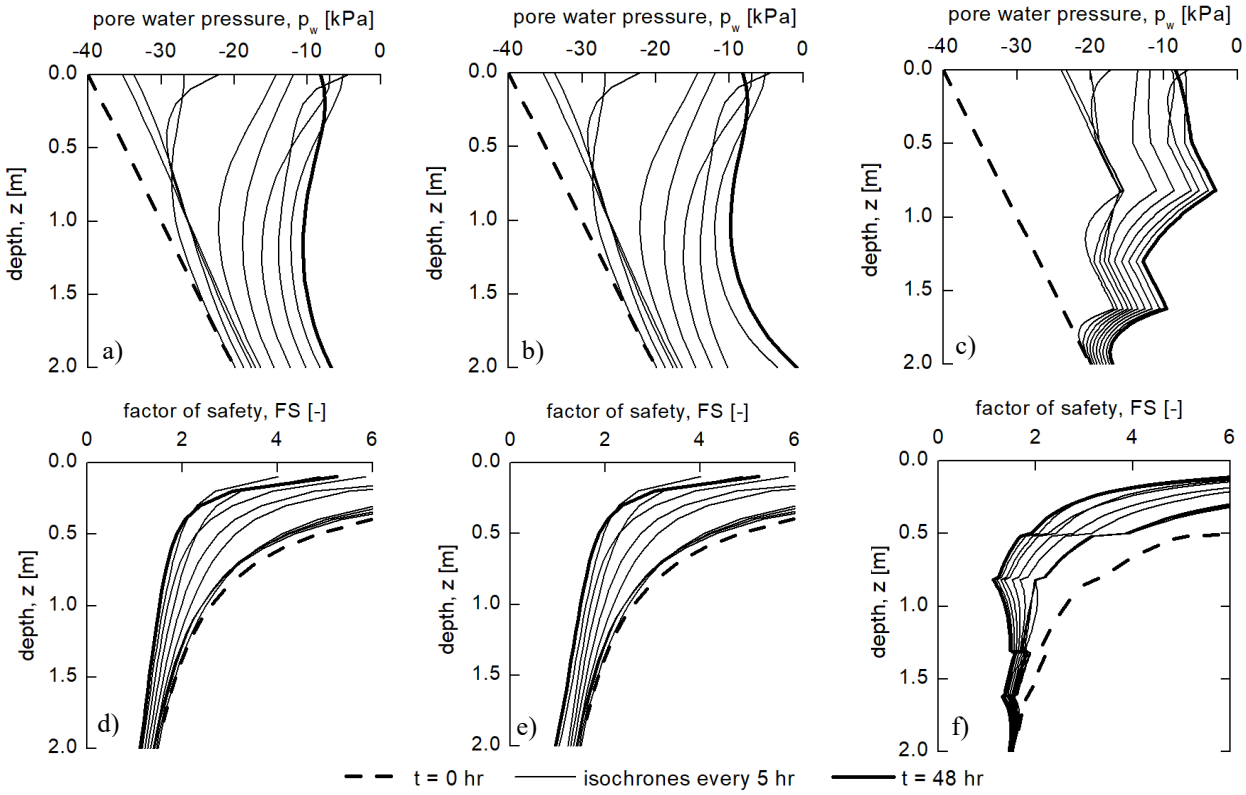

Figure 5. Computed profiles of pore pressure and Factor of Safety for: homogeneous model **H1** (a and d), homogeneous model **H2** with bedrock spring (b and e) and layered model **L** (c and f).

The computed profiles of pore pressure p_w, and FS (for a typical slope angle of 40°) for model **H1** are shown in Figure 5a and 5d, respectively. The simulation shows that the most critical zone is located at the base, where a value of p_w = -8kPa leads to a FS = 1.1 by the end of the storm. The results for model **H2** are similar (Figure 5b and 5e) until the exfiltration rate is applied (see last two isochrones), resulting in an unstable scenario (FS <1) at t= 40 hr. For the layered model **L** (Figure 5c and 5f), the simulations indicate the development of spikes of p_w at the interfaces between each layer. In this case, failure is reached at t = 48 hr and at a depth z = 0.8 m, with a correspondent value of p_w = -2.5 kPa.

The previous results can be better visualized in terms of time series as shown in Figure 6. The input rainfall is shown in Figure 6a, while the computed temporal evolution of p_w at the ash/pumice interface (z = 0.8 m, for the layered model **L**), and at the bedrock (z = 2.0 m for homogeneous models **H1** and **H2**) are shown in Figure 6b. The results indicate that only the model scenarios **L** and **H2** provided values of FS<1 during the reported time interval of landslide triggering (Figure 6c). This suggests that the sole analysis of the failure time provides limited support to justify the validity of such hypotheses. In fact, different combinations of slope thickness, inclination, and initial conditions could lead to different landslide triggering times. In order to analyze this, the following section describes each of the model scenarios in terms of landslide susceptibility maps.

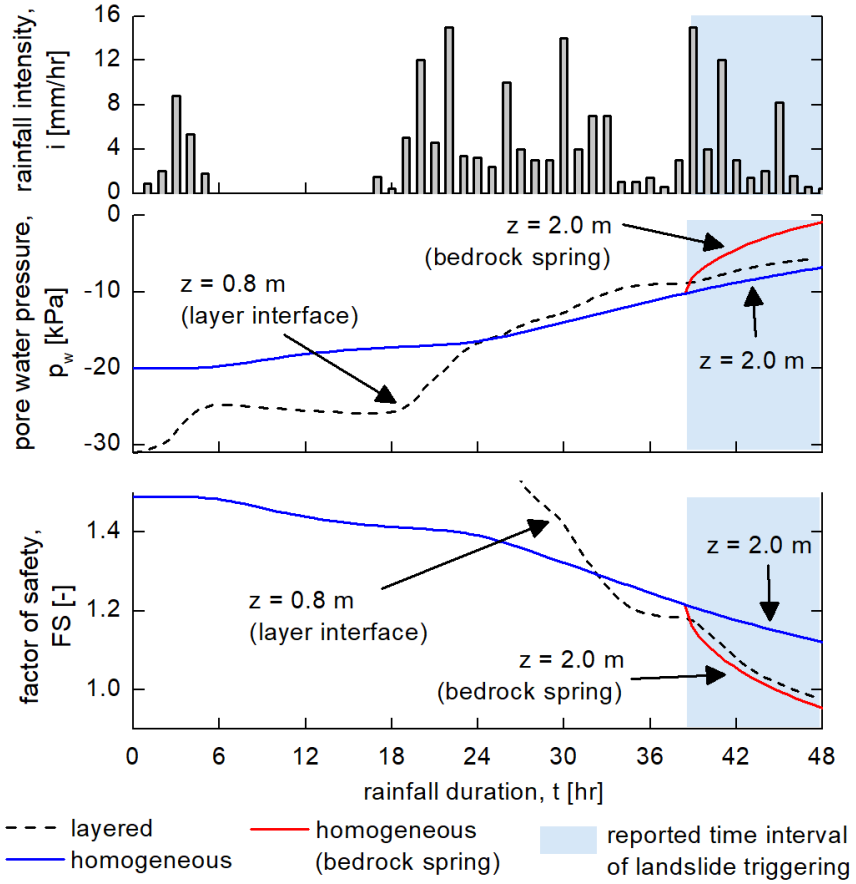

Figure 6. Input rainfall, and computed time series of pore pressure and Factor of Safety

ANALYSIS OF RESULTS

The computed landslide susceptibility map (at t=48 hr) for model **H1** is shown in Figure 7. Each colored pixel is associated with a computed unstable cell (FS<1). To allow better visual inspection, three insets are shown at higher spatial resolution. These are located at the western, central, and eastern part of the landscape. Visual comparison between documented landslide source areas (red polygons) and computed unstable zones indicates a poor spatial model performance in the western and central parts of the study zone. Indeed, nil values of success index, SI (a performance metric quantifying the ratio of predicted unstable areas matching the reported landslide contours; Sorbino et al., 2010) were obtained for 33 landslides (out of 47), thus corroborating that the assumption of homogeneous slopes cannot adequately explain the widespread distribution of failures over the entire zone of study.

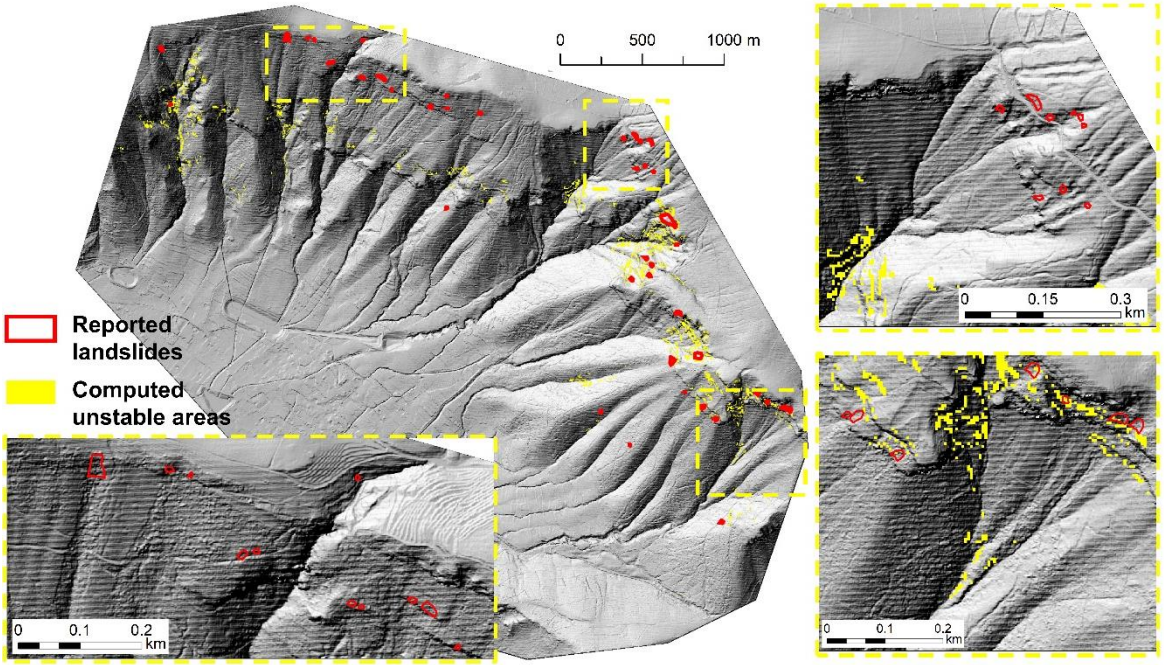

Figure 7. Computed susceptibility map for model H1.

The results for model **H2** are shown in Figure 8. This simulation results in a larger amount of unstable area across the landscape due to the activation of bedrock springs. Specifically, there is significant amount of overpredictions in the central portion of the massif. Indeed, the ratio of SI versus overpredictions (i.e., false positives), often used to measure the spatial performance of such models (Lizarraga et al., 2017) is about 5, while in the previous case is close to 7. In other words, while the introduction of bedrock exfiltration helped to improve the amount of successful computations in sectors that were not captured by the model **H1** (compare insets of Figure 7 and 8), such result came at the expense of a larger overpredicted area.

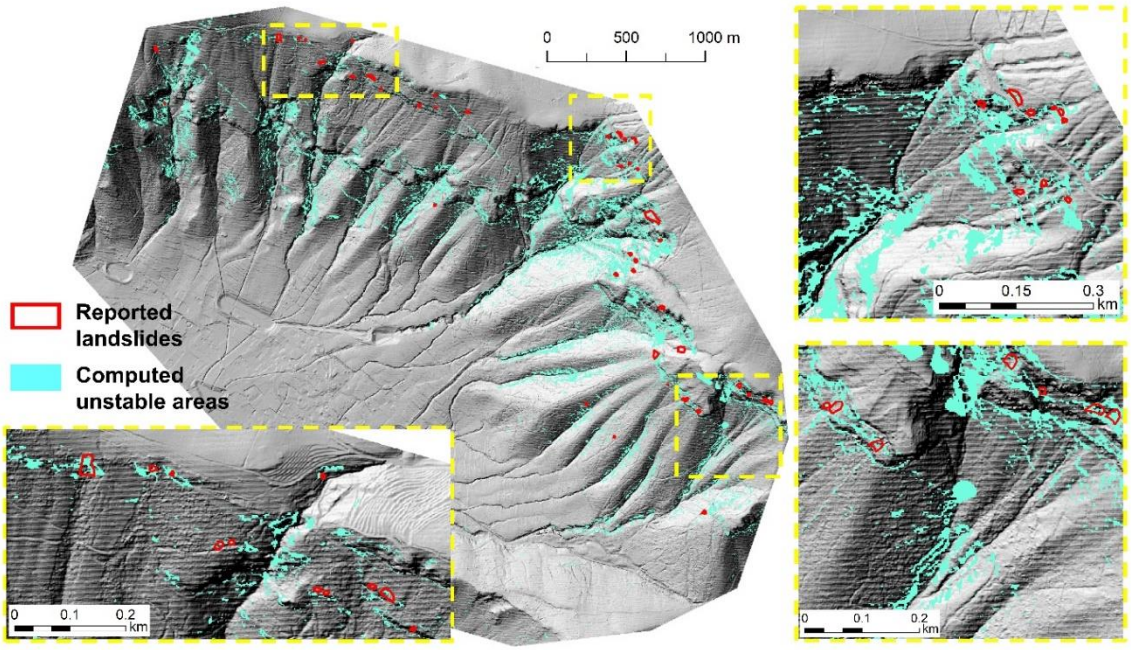

Figure 8. Computed susceptibility map for model H2 (including bedrock exfiltration).

The computed susceptibility map for model scenario **L** is shown in Figure 9. Direct visual inspection between the documented landslide areas and the computed unstable zones suggests a good spatial performance of the model across the landscape. Specifically, 30 out of 47 landslides were characterized by values of SI>50%, resulting in an overall ratio SI/EI close to 10. This indicates that the sole presence of layering greatly improves the performance of the computations even when the adopted stratified sections are based on simplified averaged profiles that are homogeneously distributed across the domain.

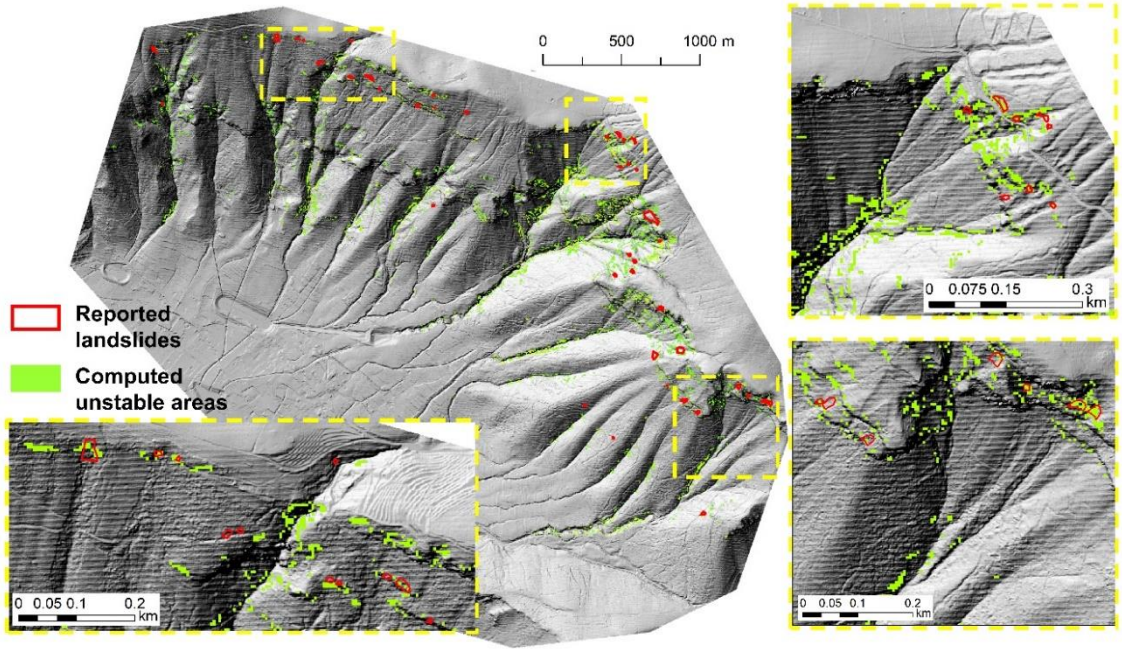

Figure 9. Computed susceptibility map for model L.

The previous susceptibility maps were obtained for t = 48hr. To obtain an assessment of the temporal performance of the model across the region, the time evolution of computed unstable area for each model is shown in Figure 10. By the end of the storm, model **H2** results in more than twice the unstable area than model **L**. Additionally, the effects of bedrock exfiltration are clearly seen after t=38 hr, when the spring is activated, leading to a higher rate of computed instabilities. Indeed, model scenario **H2** reaches the same amount of unstable area that model **L** by t=40hr.

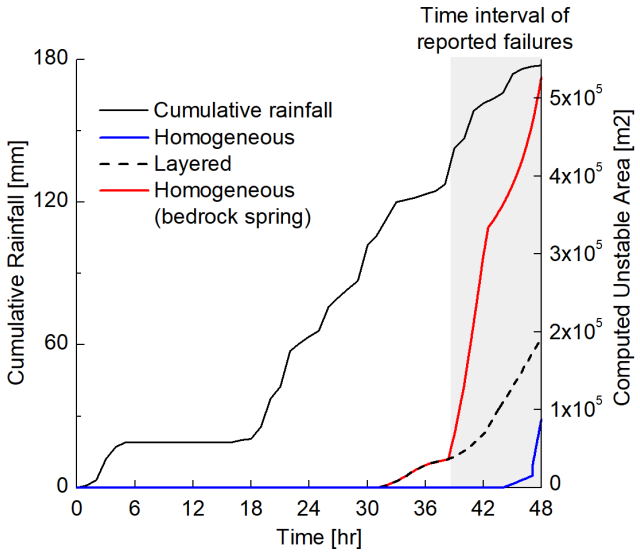

Figure 10. Comparison between temporal evolution of computed unstable area for each model.

These results highlight the crucial effect of layering on landslide triggering. Further evidence that may support such hypothesis are the distribution of failure depths observed by some authors in the field (Crosta and Dal Negro, 2003) which were mostly reported at shallow interfaces between ash and pumices. In the context of model simulations, while the hypothesis of bedrock exfiltration promotes primarily the development of basal failures, in layered profiles instabilities can develop both at soil interfaces and at the base (Lizárraga and Buscarnera, 2018). Such considerations suggest that, although some evidence indicates that failure at soil-bedrock interfaces can play an important role (Cascini et al., 2011) and may be necessary to explain the mechanics of initiation at specific source areas, the spatially erratic and discontinuous nature of exfiltration sources implies that they should be carefully mapped and inserted only at specific locations to use them accurately in spatially-distributed models.

CONCLUSIONS

This work described the application of a spatially-distributed model for landslide susceptibility zonation. The model focuses on regions prone to shallow landsliding in unsaturated deposits. To this aim, a description of a case study involving a series of documented landslides in unsaturated volcanic soils was first introduced. Different scenarios were tested to back-analyze the spatial and temporal occurrence of the events, namely, i) slope failure caused by infiltration in homogenous deposits, ii) failures promoted by contrasts in permeability within heterogeneous profiles, and iii) instabilities taking place in correspondence of bedrock springs in homogeneous slopes. The results were evaluated by comparing the computed susceptibility maps and temporal evolution of unstable area against the documented landslide inventory. It was shown that the sole use of homogeneous

profiles could not explain the observed spatial and temporal evidence of landslide triggering over the whole study area. The introduction of bedrock exfiltration can help to capture events that were not predicted by the homogeneous model; however, the extreme assumption of pervasively distributed springs leads to lower values of performance indicators (SI/EI ratio). Alternatively, the use of stratified profiles leads to an improved spatiotemporal performance over the entire zone of study, thus suggesting that layering played a predominant role on the observed widespread distribution of landslide triggering.

ACKNOWLEDGEMENTS

This work was supported by the National Science Foundation under Grant No. ICER-1854951.

REFERENCES

Bilotta, E., Cascini, L., Foresta, V., and Sorbinow, G., 2005, Geotechnical characterisation of pyroclastic soils involved in huge flowslides: Geotechnical & Geological Engineering, v. 23, no. 4, p. 365-402.

Cascini, L., Cuomo, S., and Della Sala, M., 2011, Spatial and temporal occurrence of rainfall-induced shallow landslides of flow type: A case of Sarno-Quindici, Italy: Geomorphology, v. 126, no. 1, p. 148-158.

Cascini, L., & Sorbino, G. (2003). *The contribution of soil suction measurements to the analysis of flowslide triggering.* Paper presented at the Workshop ‘‘Flows.

Crosta, G., and Dal Negro, P., 2003, Observations and modelling of soil slip-debris flow initiation processes in pyroclastic deposits: the Sarno 1998 event: Natural Hazards and Earth System Science, v. 3, no. 1/2, p. 53-69.

De Vita, P., Agrello, D., and Ambrosino, F., 2006, Landslide susceptibility assessment in ash-fall pyroclastic deposits surrounding Mount Somma-Vesuvius: Application of geophysical surveys for soil thickness mapping: Journal of Applied Geophysics, v. 59, no. 2, p. 126-139.

Godt, J., Baum, R., Savage, W., Salciarini, D., Schulz, W., and Harp, E., 2008, Transient deterministic shallow landslide modeling: requirements for susceptibility and hazard assessments in a GIS framework: Engineering Geology, v. 102, no. 3, p. 214-226.

Guadagno, F., Forte, R., Revellino, P., Fiorillo, F., and Focareta, M., 2005, Some aspects of the initiation of debris avalanches in the Campania Region: the role of morphological slope discontinuities and the development of failure: Geomorphology, v. 66, no. 1, p. 237-254.

Frattini, P., Crosta, G. B., Fusi, N., & Dal Negro, P. (2004). Shallow landslides in pyroclastic soils: a distributed modelling approach for hazard assessment. *Engineering Geology*. *73*(3-4), 277-295.

Lizárraga, J. J., Frattini, P., Crosta, G. B., and Buscarnera, G., 2017, Regional-scale modelling of shallow landslides with different initiation mechanisms: Sliding versus liquefaction: Engineering Geology, v. 228, p. 346-356.

Lizárraga, J. J., and Buscarnera, G., 2018, Spatially-distributed modelling of rainfall-induced landslides in shallow layered slopes: submitted to Landslides.

Mancarella, D., Doglioni, A., and Simeone, V., 2012, On capillary barrier effects and debris slide triggering in unsaturated layered covers: Engineering geology, v. 147, p. 14-27.

Montgomery, D. R., and Dietrich, W. E., 1994, A physically based model for the topographic control on shallow landsliding: Water resources research, v. 30, no. 4, p. 1153-1171.
Petley, D., 2012, Global patterns of loss of life from landslides: Geology, v. 40, no. 10, p. 927-930.
Pirone, M., Papa, R., Nicotera, M. V., and Urciuoli, G., 2015, In situ monitoring of the groundwater field in an unsaturated pyroclastic slope for slope stability evaluation: Landslides, v. 12, no. 2, p. 259-276.
Sorbino, G., Sica, C., & Cascini, L. (2010). Susceptibility analysis of shallow landslides source areas using physically based models. *Natural Hazards*. *53*(2), 313-332.